

https://doi.org/10.1070/QEL17183

Experimental studies of 1.5–1.6 μm high-power single-frequency semiconductor lasers

O.O. Bagaeva, R.R. Galiev, A.I. Danilov, A.V. Ivanov, V.D. Kurnosov, K.V. Kurnosov, Yu.V. Kurnyavko, M.A. Ladugin, A.A. Marmalyuk, V.I. Romantsevich, V.A. Simakov, R.V. Chernov, V.V. Shishkov

Abstract. **High-power semiconductor laser systems based on 1.5–1.6 μm single-frequency distributed feedback (DFB) lasers with a sidewall Bragg diffraction grating are developed and their current–voltage, light–current, and spectral characteristics are experimentally studied. The characteristics of conventional lasers with a Fabry–Perot cavity and DFB lasers fabricated from one and the same heterostructure are compared. At a pump current not exceeding 700 mA, a conventional laser with a cavity length of 1.6 mm and a mesa-stripe width of 3 μm emits a power no lower than 200 mW versus 150 mW of the DFB laser; both lasers are mounted in a housing 11 mm in diameter. The DFB laser mounted in a butterfly housing emits a power no lower than 100 mW at the exit of the single-mode cable at a pump current not exceeding 500 mA, which, at a 60% coupling efficiency, corresponds to a power no lower than 165 mW; the side-mode suppression ratio in this case is no lower than 53 dB. It is shown that the wavelength deviation with changing pump current and temperature is almost an order of magnitude lower for the DFB laser than for the conventional laser.**

Keywords: *single-frequency DFB lasers, current–voltage, light–current, and spectral characteristics, wavelength 1.5–1.6 μm, Bragg grating.*

1. Introduction

At present, interest in high-power single frequency distributed feedback (DFB) lasers emitting in the wavelength range 1400–1600 nm has sharply increased. These lasers are widely used in telecommunications, coherent fibre-optic communication lines with wavelength division multiplexing, fibre-optic sensors, high-resolution laser spectroscopy, frequency standards, scientific engineering, etc.

Takaki et al. [1] considered 1.55 μm lasers for communication systems with wavelength division multiplexing and for transmission of cable television signals. The laser structures comprising a buried heterostructure (BH) based on the InGaAsP/InP were grown by MOCVD (stripe contact width 2 μm, crystal length 400–800 μm). At a cavity length of 800 μm and an output power not exceeding 100 mW, the laser linewidth was 0.8 MHz and the relative intensity noise (RIN) was less than –160 dB Hz^{-1}.

The lasers for analogue signal transmission described in [2] had a side mode suppression ratio (SMSR) exceeding 50 dB, a maximum output power of 130 mW, and a RIN below –160 dB Hz^{-1} in the frequency range 0.4–20 GHz. The laser radiation was coupled out using a polarisation-maintaining fibre.

Huang et al. [3] reported on the development of a 1550 nm laser with an output power of 140 mW at a pump current of 400 mA with a RIN below –161 dB Hz^{-1} and a narrow (below 155 kHz) radiation line. According to this work, this laser can be used for signal transmission in communication lines up to 100 km long. The operation time of the laser exceeded 8800 h with an increase in the pump current no larger than 10%. The extrapolated lifetime of the laser at a temperature of 25 °C was 28.3 years at an activation energy of 0.8 eV.

The BH lasers considered in [4] had an output power of 200 mW at a RIN not exceeding –165 dB Hz^{-1} and an SMSR above 50 dB. It was shown that the BH lasers have a considerably lower noise and a wider range of modulation frequencies than ridge lasers.

High-power low-RIN directly modulated 1.55 μm lasers for analogue signal transmission were considered in [5]. The output laser power was 140 mW at a pump current of 550 mA, a RIN of –157 dB Hz^{-1}, and an SMSR exceeding 55 dB. The modulation band exceeded 7 GHz and the slope efficiency was 0.34 W A^{-1} at a pump current of 350 mA, a stripe width of 3.5 μm, and a crystal length of 1 mm. The active region of the laser contained nine undoped quantum wells.

A 1.55 μm DFB laser with a sidewall diffraction grating in the AlGaInAs/InP system was developed in [6]. Stable single-mode operation of the laser with an SMSR exceeding 45 dB was demonstrated. The operation of a similar laser in the InGaAs/GaAs/AlGaAs system was considered in [7].

To achieve selective feedback in a laser, it was proposed in [8] to form in one of the emitters a deep (about 3 μm) diffraction grating with a long (2 μm) period, which corresponds to the maximum reflection coefficient in the 12th diffraction order. These gratings have been created.

In the present work, we report on the development of a single-frequency ridge laser with a side (laterally coupled) first-order diffraction grating for the emission wavelength of 1.5–1.6 μm similar to the lasers described in [5, 6]. The diffraction grating was fabricated using electron-beam lithography at the V.G. Mokerov Institute of Ultrahigh Frequency Semiconductor Electronics, Russian Academy of Sciences, while the growth of the hetero-

O.O. Bagaeva, A.I. Danilov, A.V. Ivanov, V.D. Kurnosov, K.V. Kurnosov, Yu.V. Kurnyavko, M.A. Ladugin, A.A. Marmalyuk, V.I. Romantsevich, V.A. Simakov, R.V. Chernov, V.V. Shishkov OJSC M.F. Stel'makh Polyus Research Institute, ul. Vvedenskogo 3/1, 117342 Moscow, Russia; e-mail: webeks@mail.ru;
R.R. Galiev V.G. Mokerov Institute of Ultrahigh Frequency Semiconductor Electronics, Russian Academy of Sciences, Nagornyi pr. 7, stroenie 5, 117105 Moscow, Russia

Received 11 November 2019
Kvantovaya Elektronika **50** (2) 143–146 (2020)
Translated by M.N. Basieva

structures (HS's), fabrication of the active element, assembling of the lasers, and the study of their parameters were performed at OJSC M.F. Stel'makh Polyus Research Institute.

The DFB laser fabrication process usually includes two cycles, namely, the growth of the required HS and the profiling of the Bragg grating [9]. To complete the fabrication of a laser structure, it is necessary to cover the open grating surface by a semiconductor material using epitaxial overgrowth, which is related to some technological problems leading to defect formation. These disadvantages can be avoided by using a technique similar to that used in [5, 6], which is based on the fabrication of a longitudinal Bragg grating located on the active region sides and optically coupled with this region. The growth of heterostructures, the geometry of layers, and the results of investigation of the current–voltage (I–V), light–current (L–I), and spectral characteristics of conventional high-power 1.5–1.6 μm semiconductor lasers with a Fabry–Perot cavity are described in detail in [10].

In the present work, we formed on the grown HS a 2.5–3 μm-wide mesa-stripe with the etching depth not reaching the waveguide layer by 0.15 μm (the active region was not etched). Then, to the right and left from the mesa-stripe, we formed a first-order Bragg grating by electron-beam lithography with a $\lambda/4$ shift and a period in the range 230–250 nm depending on the HS parameters. The average period accuracy was 0.1 nm, and the coherence in the groove pattern was retained at a distance no less than 10 mm. The grating etching depth varied from 60 to 250 nm.

Next, we performed standard fabrication of the active laser element, which included deposition of dielectric layers, photolithography, metallisation, etc. As an insulating layer, we used a silicon nitride film. The DFB laser cavity length was 1.6 mm. The plane-parallel cavity faces were coated with reflection and antireflection films with reflection coefficients of ~100% and 5%, respectively. An electron microphotograph of the heterostructure with a mesa-stripe and a Bragg grating is shown in Fig. 1. The laser diode (LD) characteristics were measured from the cavity face with the 5% reflection. We used no any methods of suppression of parasitic feedback due to reflection from faces. All devices were mounted the active region up. The laser diode crystals in housings 11 mm in diameter were soldered on a copper heat sink, while the diodes in butterfly housings were soldered on a copper–tungsten thermal compensator.

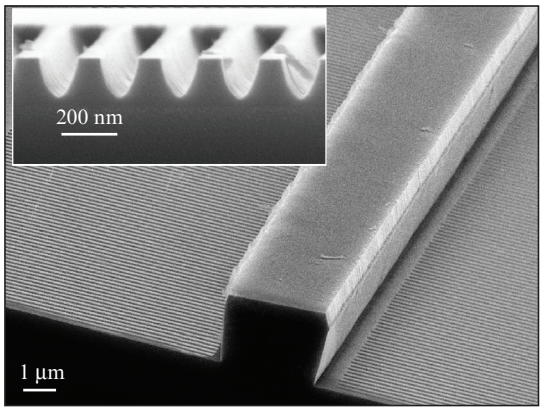

Figure 1. Electron microphotograph of a heterostructure with a mesa-stripe and a Bragg grating. The inset shows the grating cross section.

2. Characteristics of conventional and DFB lasers

To calculate the grating period, it is necessary to know the lasing wavelength of the laser fabricated from the grown HS, because accompanying documents usually give the wavelength only of electroluminescence. Therefore, HS's are usually divided into four parts, one of which is spent on the fabrication of a conventional mesa-stripe laser. After determination of the lasing wavelength and calculation of the grating period, the remained part of the HS is used for fabrication of a DFB laser. It is interesting to analyse how the characteristics of conventional lasers and lasers with diffraction gratings made of one and the same HS change with temperature. The lasers of both types were installed in housings 11 mm in diameter and mounted on a heat sink, whose temperature was controlled by an electronic circuit [10]. The results presented below correspond to the temperature range 20–50 °C.

Figure 2 shows the I–V and L–I curves of conventional and DFB lasers. Comparison of the L–I curves given in Figs 2a and 2b shows that the scatter in the characteristics of the DFB laser with temperature is considerably smaller than that of the conventional laser, but the maximum output power of conventional lasers is higher. The output power of the conventional laser at a temperature of 20 °C and pump current I = 700 mA exceeds 200 mW, while the power of the DFB laser reaches only 150 mW. The slope efficiency in the range 20–50 °C is 0.34–0.4 and 0.22–0.3 mW mA^{-1} for the conventional and DFB lasers, respectively. It is also necessary to note a decrease in the lasing threshold of the DFB laser with respect to the conventional laser.

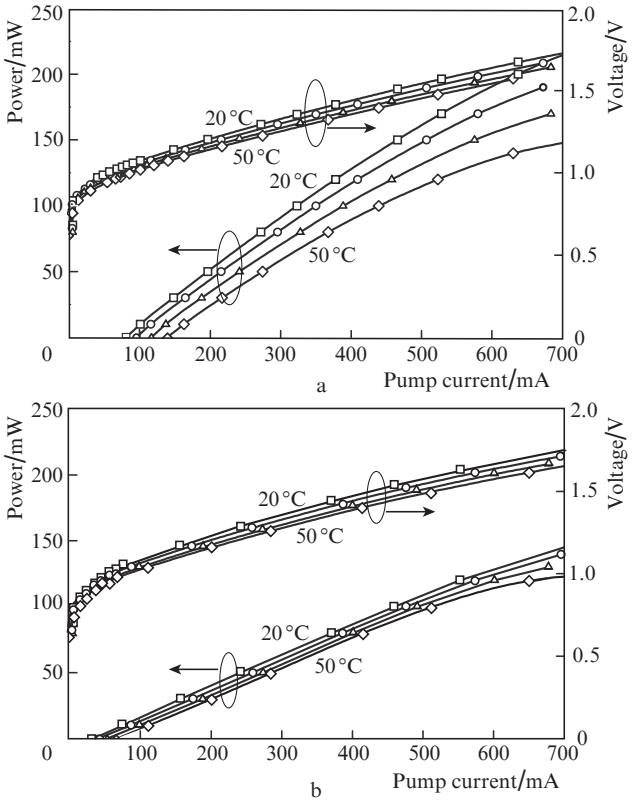

Figure 2. Current–voltage and light–current characteristics of (a) conventional and (b) DFB lasers for temperatures of 20, 30, 40, and 50 °C.

Comparison of the $I-V$ curves of the lasers shows that, despite many additional technological operations involved in the fabrication of DFB lasers, the DFB laser voltage is only slightly higher than that for conventional lasers. The dynamic resistances of conventional and DFB lasers are approximately identical and equal to 1 Ω at the working point 500 mA.

Figure 3 presents the dependences of laser wavelength λ on pump current I in the temperature range 20–50 °C for the conventional and DFB lasers. As the lasing wavelength of the conventional laser, we used the wavelength corresponding to the maximum of the laser spectrum. One can see that the temperature dependences of the wavelengths of these lasers are considerably different. Calculations yield $\Delta\lambda/\Delta I = 0.032$ nm mA^{-1} and $\Delta\lambda/\Delta T = 0.67$ nm °C^{-1} for the conventional laser, while the corresponding values for the DFB laser are $\Delta\lambda/\Delta I = 0.0043$ nm mA^{-1} and $\Delta\lambda/\Delta T = 0.09$ nm °C^{-1}, i.e., almost an order of magnitude lower.

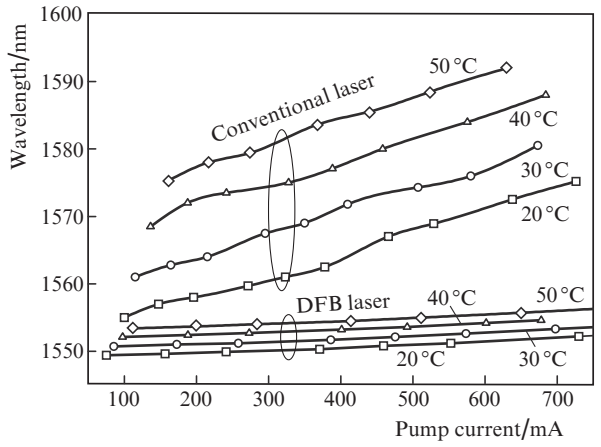

Figure 3. Dependences of the wavelength of conventional and DFB lasers on the pump current in the temperature range 20–50 °C.

The laser spectra were measured using an AQ6319 optical analyser (Yokogawa) with a spectral resolution of 0.1 Å. The laser spectrum (on a linear scale) of the conventional laser at a pump current of 500 mA is presented in Fig. 4a, which demonstrates that the spectrum consists of many modes. Figure 4b shows the DFB laser spectrum on a logarithmic scale at a current of 500 mA as well. One can see that the spectrum consist of one mode and the SMSR is ~55 dB. As SMSR, we took the ratio between the lasing mode amplitude and the maximum amplitude of the closest mode to the right or left of the lasing mode. Comparison of these spectra shows the advantage of the DFB lasers over conventional ones.

Figure 5 presents the dependences of SMSR on the pump current within the temperature range 20–50 °C for two different DFB lasers made of one and the same HS. One can see that an increase in temperature to 50 °C leads to a decrease in the SMSR for the laser in Fig. 5a and, vice versa, to an increase in the SMSR for the laser in Fig. 5b. We failed to explain the reasons for this difference in the behaviour of the lasers.

The measurements of the angular beam divergence for the conventional laser at a temperature of 20 °C and a power of 50 mW showed that the beam divergence is 46.5° in the plane

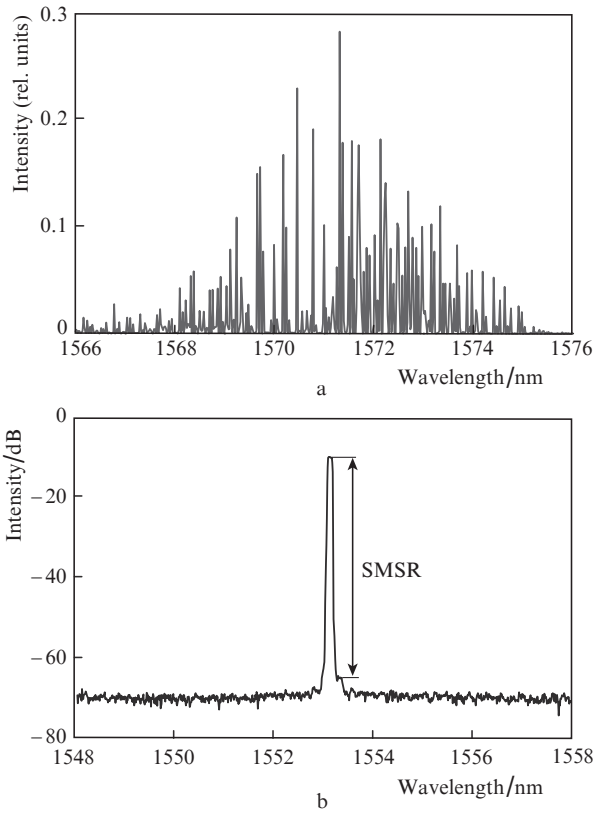

Figure 4. Spectra of the (a) conventional laser on a linear scale and (b) DFB laser on a logarithmic scale at a pump current of 500 mA.

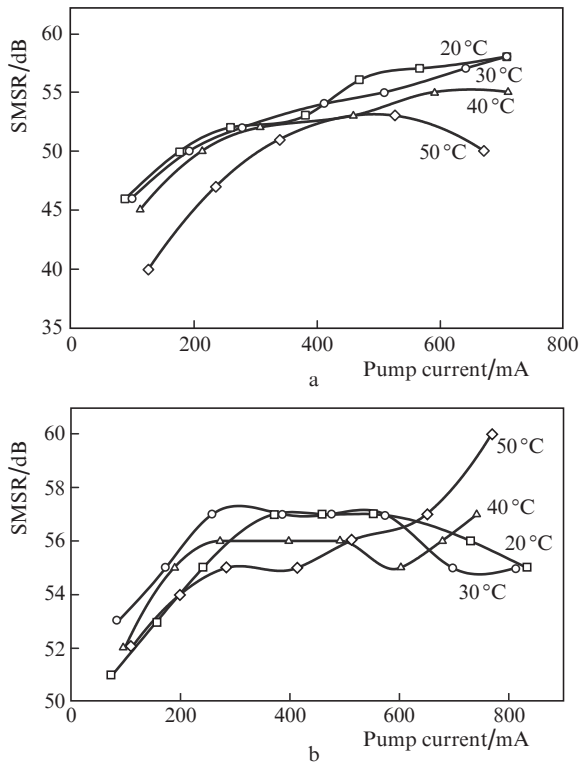

Figure 5. Dependences of the SMSR of two DFB lasers fabricated of one and the same heterostructure on the pump current in the temperature range 20–50 °C.

perpendicular to the p–n junction and 8.7° in the plane parallel to the p–n junction. These values for the DFB laser are 45.6° and 10.6°, respectively. Thus, the beam divergence in the plane perpendicular to the p–n junction is almost identical, while the divergence in the plane parallel to the p–n junction is somewhat higher for the DFB laser due to, probably, the presence of a grating. Similar values of the angular divergence in the plane perpendicular to the p–n junction were reported in [10].

Figure 6 presents the L–I curve of the DFB laser in a standard butterfly housing at a temperature of 20 °C, which was measured at the exit of the single-mode fibre cable. The laser power was 100 mW at a pump current not exceeding 500 mA, and the slope efficiency was 0.26 mW mA^{-1}. The efficiency of coupling into the single-mode fibre cable was approximately 60%, which allows us to conclude that the laser power exceeded 165 mW. The SMSR at pump currents exceeding 200 mA was no lower than 53 dB, while the relative intensity noise did not exceed –160 –170 dB Hz^{-1} at a frequency of 5 GHz.

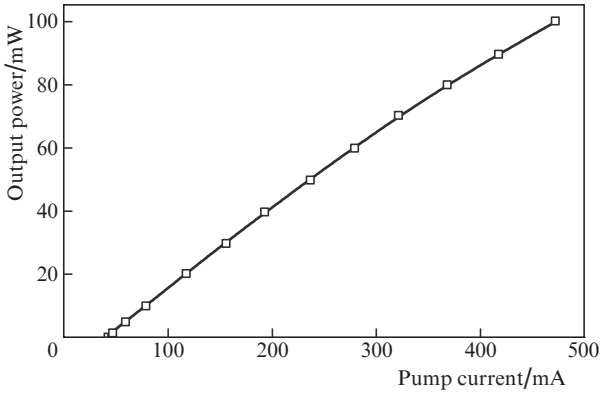

Figure 6. Light–current characteristic of the DFB laser in a butterfly housing.

The dependences of the wavelength and SMSR of the DFB laser in a butterfly housing on the pump current are presented in Fig. 7. One can see that the $\lambda(I)$ dependence deviates from linear with increasing pump current due to a rise in the temperature of the active laser region. In particular, $\Delta\lambda/\Delta I = 2.1 \times 10^{-3}$ nm mA^{-1} in the pump current range 100–150 mA and $\Delta\lambda/\Delta I = 3.35 \times 10^{-3}$ nm mA^{-1} in the range 380–480 mA, which almost coincides with the measured results for lasers in housings 11 mm in diameter.

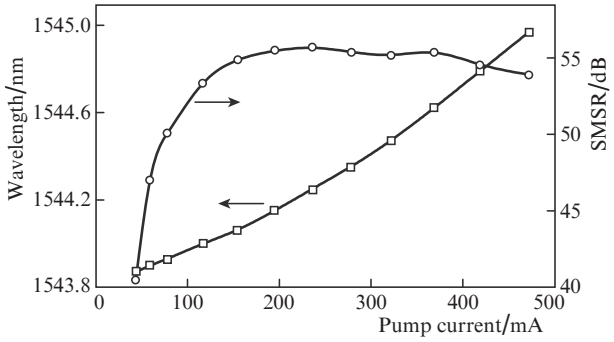

Figure 7. Dependences of the wavelength and SMSR of the DFB laser in a butterfly housing on the pump current.

The lifetime tests of the DFB lasers performed at a temperature of 55 °C showed that the extrapolated lifetime of the lasers at a temperature of 25 °C is no shorter than 100000 h at the activation energy $E_a = 0.6$ eV.

Thus, we have developed a technology of fabrication of high-power single-frequency DFB lasers ($\lambda = 1.5 - 1.6$ μm) with a sidewall Bragg diffraction grating and experimentally studied their characteristics.

The output power of the DFB lasers with a cavity length of 1.6 mm and a mesa-stripe width of 3 μm mounted in a housing 11 mm in diameter was no lower than 150 mW at a pump current not exceeding 700 mA.

The laser power at the exit from the single-mode fibre cable at a pump current not exceeding 500 mA was no lower than 100 mW. It is shown that the change in the laser wavelength with changing pump current and temperature is almost an order of magnitude lower for the DFB lasers than for conventional lasers with a Fabry–Perot cavity. The extrapolated lifetime of the lasers for a temperature of 25 °C is no shorter than 100000 h (at $E_a = 0.6$ eV).

References

1. Takaki K., Kise T., Maruyama K., Hiraiwa K., et al. *Furukawa Review*, **23**, 1 (2003).
2. Burie J.R., Beuchet G., Mimoun M., Pagnod-Rossiaux P., et al. *Proc. SPIE*, **7616,** 76160Y (2010).
3. Huang J.S., Lu H., Su H. *IEEE LEOS* (Newport Beach, CA, 2008) paper ThBB-3, p. 894.
4. Zhao Y.G., Nikolov A., Dutt R. *Proc. SPIE,* **7933**, 79332J (2011).
5. Faugeron M., Tran M., Lelarge F., et al. *IEEE Photonics Techn. Lett*., **24**, 116 (2012).
6. Wang J.W., Tian J.B., Cai P.F., et al. *IEEE Photonics Techn. Lett*., **17**, 1372 (2005).
7. Martin R.D., Forouhar S., Keo S., et al. *IEEE Photonics Techn. Lett*., **7**, 244 (1995).
8. Vasil'eva V.V., Vinokurov D.A., Zolotarev V.V., Leshko A.Yu., et al. *Fiz. Tekh. Poluprovodn*., **46**, 252 (2012) [*Semiconductors*, **46**, 241 (2012)].
9. Allovon M., Quillec M. *IEE Proc. J*., **139**, 148 (1992).
10. Gorlachuk P.V., Ivanov A.V., Kurnosov V.D., Kurnosov K.V., Marmalyuk A.A., et al. *Quantum Electron*., **48**, 495 (2018) [*Kvantovaya Elektron.*, **48**, 495 (2018)].